Fracture energy density of interstitial component of asphalt mixtures

FRACTURE ENERGY DENSITY OF INTERSTITIAL COMPONENT OF ASPHALT MIXTURES

Yu Yan [a]* — Francesco Preti [b] — Elena Romeo [b] — George Lopp [a] — Gabriele Tebaldi [b] — Reynaldo Roque [a]

[a] *Department of Civil and Coastal Engineering, University of Florida, Gainesville, USA*

[b] *Department of Engineering and Architecture, University of Parma, Parma, Italy*

* *Corresponding author. 365 Weil Hall P.O. BOX 116580, University of Florida, Gainesville, FL 32611, Email: sayme@ufl.edu*

ABSTRACT.

Interstitial component (IC), referring to the finer portion of asphalt mixture, is primarily responsible for tensile properties and thereby strongly affects mixture cracking performance. Whereas mixture tests are usually complex and labor-intensive, determination of fracture properties with a simpler test on the IC portion will add values in terms of ranking mixtures and predicting mixture fracture properties. An interstitial component direct tension (ICDT) test, which was derived from the dog bone direct tension test originally developed for asphalt mixtures, was applied to determine the fracture energy density (FED) of mixture IC portion. FED describes the damage tolerance before fracture occurs and it is also a component associated with crack propagation. Two methods of strain determination were evaluated including a digital image correlation (DIC) system and a predictive equation derived from finite element analysis with load-head displacement as input. ICDT tests were conducted on the IC portion of two sets of four mixtures, which had identical coarse aggregate structure. The DIC system yielded greater failure strain than those based on load-head displacement. However, the ratios between the two values for all mixtures were almost constant, supporting the use of the predictive equation as a surrogate. Moreover, IC FED ranked these mixtures in the same order as mixture FED and more importantly, an excellent correlation was observed between IC FED and mixture FED of these mixtures. In conclusion, the ICDT test can be used to determine the IC FED, which provides valuable insights regarding the effect of IC characteristics on mixture FED.

Keywords: interstitial component; fracture energy density; digital image correlation; finite element analysis; damage tolerance; failure strain

1. INTRODUCTION

1.1 Background

Load-induced fatigue cracking at intermediate temperatures is a major asphalt pavement distress mode. Cracks typically originate and propagate through binder film not aggregate grains and thus, fatigue resistance of asphalt binder significantly impacts fatigue performance of asphalt mixtures (1). The parameter G*sin(delta) in the current Superpave specification has been used to describe the binder's contribution to mixture fatigue damage resistance. However, the effectiveness of this parameter is questionable primarily because its testing procedure does not introduce sufficient damage into the specimen (2). Several advanced binder cracking tests have been developed during the last decade, including the linear amplitude sweep (LAS) test, the double edge notched tension (DENT) test and the binder fracture energy (BFE) test. The LAS test consists of cyclic loading with loading amplitudes that are systematically increased to accelerate damage. LAS testing procedure includes a frequency sweep to obtain an undamaged material response and an amplitude sweep to evaluate damage evolution (3-4). The DENT test is essentially a ductility test but with two notches of controlled depth placed in the center of the specimen (5). This test can be performed to obtain the essential work of fracture as a measure of the fatigue and crack resistance behavior of asphalt binders. The BFE test is a direct tension test with an optimized specimen geometry that ensures accurate measurement of stress and strain on the fracture surface, which in turn ensures accurate fracture energy density (FED) calculation (6-7). Each of the three tests now has an AASHTO provisional standard to characterize the fatigue damage tolerance, resistance to ductile failure, and fracture tolerance of asphalt binders (8-10), respectively. Studies have also shown that binder relaxation properties, captured by the R-value from relaxation spectra, correlate with cracking performance of asphalt mixtures (11-13). Rheological parameters such as the Viscous to Elastic Transition (VET) temperature and the complex modulus at the VET temperature (G^*_{VET}) have also been successfully employed to characterize changes in properties of asphalt binder at different levels of age hardening and/or distress level (cracked or uncracked sites) (14-15).

Mixture cracking performance is also governed by factors that binder tests alone cannot account for, such as binder content and aggregate structure. Testing mixtures directly currently appears to be the only way to assess the effect of these factors on mixture cracking performance. Several mixture cracking tests are now available, including the Texas Overlay test (16-17), the semi-circular bending test (18), the Superpave indirect tension test (19-20), the bending beam fatigue test (21-22), the simplified viscoelastic continuum damage fatigue test (23-24), the disk-shaped compact tension test (25), the dog-done direct tension (DBDT) test (26), and the direct tension test (27-28). In the U.S., many of these tests have been evaluated in the NCHRP 9-57 project, but there was no consensus on the selection of an ideal cracking test for routine use (29). Outside of the U.S., the RILEM committees TC 101 and TC 152 performed the first interlaboratory tests on mixture fatigue and identified the needs for understanding and modeling the complex phenomena appearing during fatigue of bituminous mixtures (30). In response, the RILEM committee TC 182 conducted a follow-up interlaboratory campaign that evaluated eleven mixture tests (five general fatigue test specimen geometries) and different models using damage theory (31). Results indicated that the classical fatigue analysis had great limitation, but the damage approach appeared to be a rational option to characterize mixture fatigue (31-32). The European Union now has standardized the bending test on prismatic shaped specimens to evaluate the crack initiation of asphalt mixtures (33) and the semi-circular bending test to evaluate the crack propagation (34).

1.2 Research motivation

Literature indicates that binder tests alone cannot provide a complete assessment of mixture cracking performance, and although promising, these commonly used mixture tests are also known to be complex and labor-intensive. Therefore, there is a need for a simpler test that can be used to obtain properties relevant to mixture cracking performance. It is well-documented that performance of an asphalt mixture is closely related to its aggregate structure (35-36). Mixture aggregate structure can be expressed by separating the gradation into two major components: dominant aggregate size range (DASR) and interstitial component (IC) (37-38). DASR defines the size range of interactive coarse aggregate that forms the primary structural network of aggregate and provides mixture resistance to shear. IC is made up of fine aggregates, binder and air voids within the interstitial volume that bonds the coarse aggregate structure together, resisting primarily tension and, to a lesser extent, shear (38).

IC is primarily responsible for the mixture tensile properties and thereby strongly affects mixture cracking performance. IC coarseness affects the distribution of asphalt binder and the air void structure within the interstitial volume (39-40). Generally, finer IC gradations result in aggregates in closer proximity to each other, and hence, more thinly distributed asphalt binder, and smaller, less interconnected air voids, which lead to stiffer and more brittle mixtures. Conversely, coarser IC gradations result in more sparsely distributed aggregates, thus, more coarsely distributed asphalt binder, and larger, more interconnected air voids, which lead to less stiff and less brittle mixtures (39-40). Therefore, it would be of great benefit to identify or develop a test that requires small quantity of materials and short period of time for testing and data analysis to determine the fracture energy density (FED) of the mixture IC portion, which is a component that logically appears to be strongly related to the mixture FED. This would add value in terms of optimizing mixture design, ranking mixture performance and eventually predicting mixture fracture properties and performance without the need of testing mixtures.

2. OBJECTIVES

The main objective of this study was to determine the fracture energy density (FED) of the interstitial component of asphalt mixtures at intermediate temperature (10°C). Detailed objectives were as follows:

- Present the interstitial component direct tension (ICDT) test derived from the DBDT test, including the specimen geometry, specimen composition, compaction method, testing protocols and data interpretation procedure.

- Evaluate two methods of strain determination, i.e., a digital image correlation (DIC) system and a predictive equation of strain derived from finite element analysis (FEA), to obtain local strain for determination of IC FED.

- Determine the relevance and accuracy of the FED obtained from the ICDT tests by comparing the IC FED to the corresponding mixture FED.

3. SCOPE

This study adopted eight mixtures whose mixture design and mixture FED results were available from a previous study (39). Experimental factors included two aggregate types (Georgia granite and Florida oolitic limestone), one asphalt binder (PG 67-22 unmodified binder), one DASR and four IC gradations for each aggregate type. ICDT tests were conducted on the IC portion of these eight mixtures to obtain the corresponding IC fracture properties, specifically IC FED. The emphasis was to determine whether the effect of IC coarseness on mixture FED can be captured by performing the ICDT tests. Note that FED describes the damage tolerance before fracture occurs and therefore, it should only be regarded as a fracture limit and not as a complete characterization of cracking performance, which involves both crack initiation and propagation.

3.1 Mixture Gradation

Two mixtures commonly used in Florida, one with Georgia granite and one with Florida oolitic limestone, were selected as base mixtures. Identification of DASR range for both mixtures was conducted by means of particle interaction analysis, which requires the relative proportion of particles from two contiguous sieve sizes to be within 70/30 to form an interactive network (34). The granite mixture had a DASR range of 9.5 to 1.18 mm whereas the DASR of limestone mixture was broader (from 12.5 to 1.18 mm) (Supplement Figure 1). Consequently, both mixtures had the same IC range, which includes aggregates passing the 1.18 mm sieve.

To isolate the IC and its effects on mixture properties and performance, the coarse aggregate structure of the two base mixtures was kept constant and only their IC gradations were changed. This resulted in a total of eight mixtures. IC coarseness for both granite and limestone mixtures increased from IC 1 to IC 4 with IC 3 being the reference mixture (Supplement Figures 2 and 3). All mixtures were fine dense-graded and were designed following the Superpave system with 12.5 mm NMAS gradations and traffic level C, which corresponds to 3-10 million Equivalent Single Axle Loads over 20 years.

3.2 Mixture Parameters

Table 1 lists the volumetric information of the eight mixture designs. Mixtures with coarser IC required more asphalt content, resulting in higher voids in mineral aggregate (VMA) and voids filled with asphalt (VFA) values. Table 1 also summarized the mixture FED of the eight mixtures after short-term oven aging (STOA), which were determined by performing the Superpave indirect tensile (IDT) strength test. Fracture energy density (FED), which is defined as the energy per unit volume required to initiate fracture, is one of the most important failure limits of asphalt mixtures (20-21). Mixtures with a coarser IC gradation yielded greater FED, which indicates greater damage tolerance before fracture occurs. A potential explanation for this trend is that coarser IC gradation resulted in more coarsely distributed asphalt binder, and larger, more interconnected air voids, which lead to less tiff and less brittle mixtures with higher FED (39-40).

Table 1. Volumetric parameters for granite and limestone mixtures

Mixture		Air voids (V_a, %)	Total asphalt binder (P_b, %)	VMA (%)	VFA (%)	FED (kJ/m^3)
Georgia granite	IC 1	4.0	4.5	12.9	69.0	3.4
	IC 2	4.0	4.8	14.9	73.2	4.3
	IC 3	4.0	5.4	14.9	73.2	7.5
	IC 4	4.0	5.8	15.5	74.2	7.2
Florida limestone	IC 1	4.0	5.7	11.4	65.0	2.2
	IC 2	4.0	5.9	12.3	67.5	2.1
	IC 3	4.0	6.0	12.2	67.3	3.1
	IC 4	4.0	6.9	13.9	71.3	3.9

4. INTERSTITIAL COMPONENT DIRECT TENSION TEST

The ICDT test was miniaturized from the DBDT test, which was developed by Koh et al. (2009) (26) to obtain fracture properties of asphalt mixtures. Significant modification was required to adapt the DBDT concept so the resulting ICDT test would be applicable for testing interstitial component. This included scaling down the specimen geometry, determining specimen composition, developing compaction method, and identifying appropriate data collection system and associated data analysis method.

4.1 Specimen geometry

As shown in Figure 1, the geometry of ICDT specimen simulated that of the dog-bone direct tension test developed by Koh et al. (2009) (26). A scale factor of 0.5 was used for all dimensions, except that the thickness of the DBDT specimen was 5.08 cm whereas the ICDT specimen was 1.27 cm. The dog-bone geometry had high stress concentration in the middle of the specimen where stress was approximately 40% greater than that near the ends. Moreover, it introduced non-uniform stress state in middle of the specimen with the tensile stress at the outer edges about 30% greater than at its center. This resulted in a unique advantage that the failure plane was known a priori, so that stress and strain could be measured directly on the failure plane, ensuring consistent determination of FED (41).

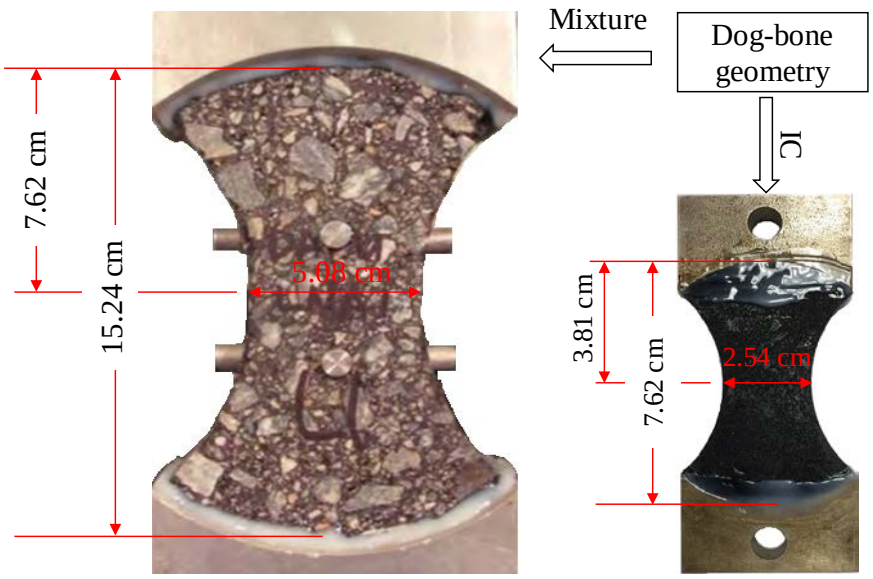

Figure 1. Dog-bone geometry for mixture and IC specimens

4.2 Specimen composition

The composition of IC component should reflect the relative volume of effective binder and IC aggregates in mixtures. The effective binder refers to the binder that is not absorbed by the DASR aggregates and the IC aggregates are aggregates that are finer than the DASR range as determined by the DASR-IC model. Therefore, the weight ratio of aggregates to total binder of the ICDT specimen is the same as the weight ratio of IC aggregates to effective binder of the corresponding mixture. Table 2 summarizes the composition of the eight mixtures and their ICDT specimens. Mixtures of the same aggregate type had the same weight of DASR and IC aggregates but different effective binder content and weight ratio of IC aggregates to effective binder. Consequently, the ICDT specimens of different mixture type had different compositions of aggregate and total binder.

Table 2. Compositions for mixture specimens and corresponding ICDT specimens

Mixture and IC specimen compositions		Mixture Superpave gyratory compacted pill				ICDT specimen		
		DASR aggregate (g)	IC aggregate (g)	Effective binder (g)	IC aggregate to effective binder	Aggregate (g)	Total binder (g)	Aggregate to total binder
Granite mixtures	IC 1	3069	1431	174	8.2	66.0	8.0	8.2
	IC 2			213	6.7	63.2	9.4	6.7
	IC 3			219	6.5	62.2	9.5	6.5
	IC 4			229	6.2	61.1	9.8	6.2
Limestone mixtures	IC 1	3015	1485	162	9.2	61.2	6.7	9.2
	IC 2			182	8.2	59.9	7.3	8.2
	IC 3			182	8.2	59.8	7.3	8.2
	IC 4			222	6.7	56.9	8.5	6.7

Knowing the volume of the ICDT specimen (32cm^3), the weight ratio of IC aggregates to effective binder of the mixture to be evaluated, and the bulk specific gravity values of aggregates and binder, the weights of aggregates and total binder of the corresponding ICDT specimen can be determined by using Equations 1 and 2. Then, the weight of aggregates was further broken up in accordance with the IC gradation of the mixture to prepare the batching sheet for ICDT specimens.

$$\frac{W_A}{W_B} = C \tag{1}$$

Where, W_A and W_B are weights of aggregate and binder of the ICDT specimen, respectively; C is the weight ratio of IC aggregates to effective binder of the mixture.

$$\frac{W_A}{G_{se}} + \frac{W_B}{G_b} = V_{ICDT} \tag{2}$$

Where, G_{se} is the effective specific gravity of IC aggregates; G_b is the specific gravity of asphalt binder; VICDT is the volume of ICDT specimen which is 32cm^3.

4.3 Specimen compaction

Loose IC mix was STOA conditioned and compacted in a stainless-steel mold using a specially designed compaction head, as shown in Figure 2. ICDT specimens were compacted to zero percent air voids because air void content and distribution (e.g., interconnected, isolated, small or large) is a mixture level factor that cannot be properly replicated or assessed by testing IC alone. ICDT specimens should be compacted to a target thickness of 1.27 cm (0.5 inch), which is the key parameter to control during compaction to obtain zero air voids.

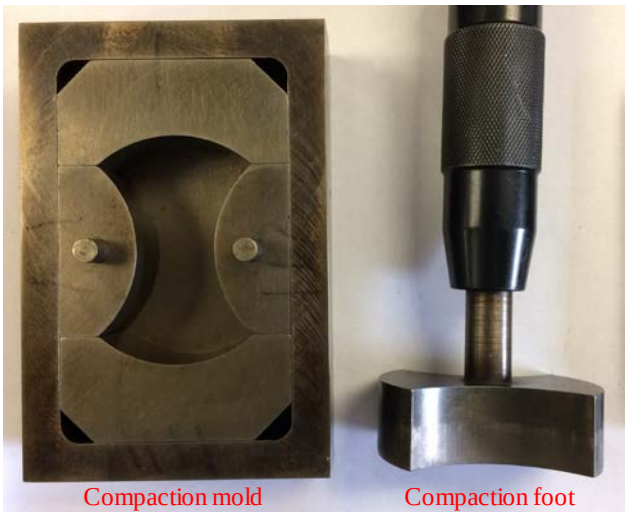

Figure 2. ICDT specimen compaction mold and steel foot

Two ICDT specimens were randomly selected for evaluation of the compaction effect. The ICDT specimen was evenly cut into three parts, on which weight and volume measurements were performed to determine their air void content. The portions close to the two heads had an average air void content of 0.8%, while the middle section had a near zero percent air void content of 0.3%. Results of density measurement were confirmed by using X-ray computed tomography. Figure 3 shows some air voids appeared to concentrate near the two heads, but no air voids were observed in the middle section where fracture occurs, and FED is determined. Even though air voids were slightly higher near the heads, fracture occurred through the middle of all specimens tested.

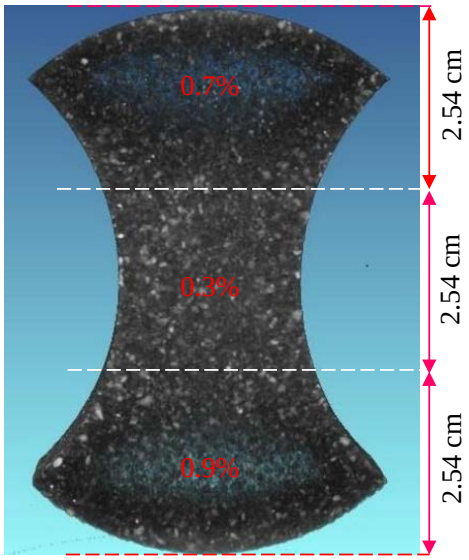

Figure 3. Distribution of air voids within the ICDT specimen determined by X-ray CT and measured air voids content of two heads and the middle section

4.4 Testing protocol

For each mixture type, six replicates with a thickness of 12.7 ±0.25 mm were prepared for testing. Epoxy was used to bond the specimen to the loading heads. To increase the effectiveness of bonding, sandpaper was used to remove the asphalt film from the top and bottom heads of the specimen. In addition, the loading heads were v-grooved to enhance bonding strength between the epoxy and loading head by increasing contact surface area.

ICDT specimens were placed in an experimental chamber set to 10°C for 2 hours before testing. The same temperature chamber was used for both conditioning and testing. The specimen was oriented vertically and aligned with the loading frame by matching the cavities of the two heads with two pins on loading frame. ICDT tests were performed at 10°C at a displacement rate of 50.8 mm/min, which were the same testing conditions used for the Superpave IDT strength test to determine the mixture FED.

4.5 Data interpretation procedure

Time, load magnitude, and load-head displacement, was measured using the material testing system (MTS) acquisition software at an adjusted rate of 2048 points per second (the test generally takes less than 2 seconds to complete). Load was transformed into average stress in the central cross-sectional area of the specimen by dividing force by the area of fracture plane, which is equal to 3.23 cm^2 (0.5 in^2). Average strain was determined by using either a digital image correlation (DIC) system or a predictive equation established between displacement and average strain using finite element analysis (FEA). The DIC system is believed to provide the most accurate local strain measurement; however, considering the cost and added complexity of the associated equipment, it was of great interest to determine whether the predictive equation could be used as a surrogate. FED is defined as the area under the stress-strain curve until the stress peak (Figure 4).

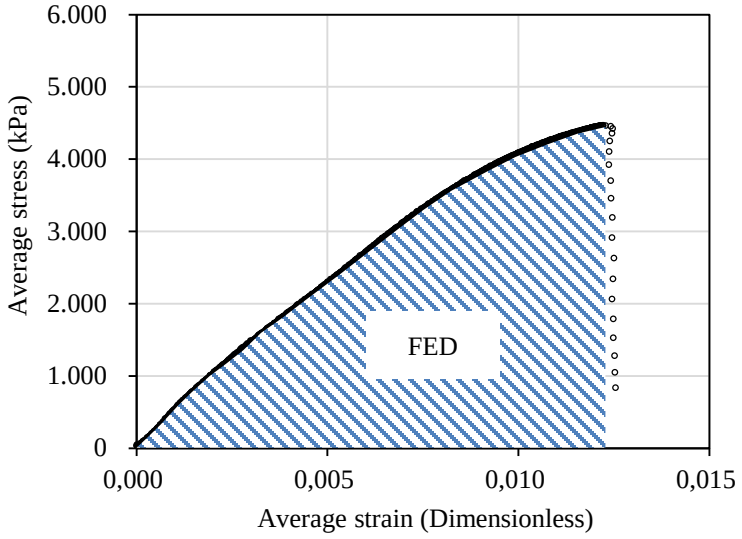

Figure 4. Determination of IC fracture energy density

4.5.1 Strain determination using digital image correlation (DIC)

The DIC system was adopted as a non-contact measurement tool to investigate the strain distribution and the instant of fracture of the ICDT specimens. Crack initiation and propagation was visualized by plotting the strain development in a color scale. Once the location and instant of fracture was determined, the system was used to obtain the strain values on the failure plane to determine the IC FED. The DIC system has two main components: a high-speed camera to acquire a sequence of images of the specimen surface during loading and an imaging process software to obtain data of interest (in this case, the local displacement and corresponding strain) (42). Figure 5 illustrates the ICDT test setup with a high-speed camera in front of an ICDT specimen been placed on the loading frame inside the environmental chamber.

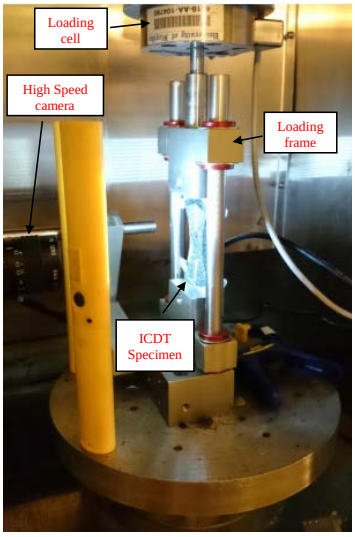

Figure 5. ICDT test setup

The basic principle of DIC is the tracking of the same points (or pixels) between two or more consecutive images. The specimen surface facing the camera was treated using white paint to create a well-contrasted and homogeneous randomly oriented texture. In this case, white paint was sprayed on either the front or the back surface of a ICDT specimen. The grey values of a deformed image (slave image) are statistically compared to an un-deformed image (master image). This step can determine the displacement of any feature location relative to its original position and estimate the corresponding strain by using a technique called area-based matching. Details regarding the DIC system can be found in work by Romeo (42).

There are three main steps associated with the analysis of images for determination of strain on the fracture plane (Supplement Figure 4). Step 1 is the selection of the region of interest (ROI), which is then meshed regularly (e.g., 10×10) in horizontal and vertical directions. Displacement used to determine the strain is computed as the difference of the feature location between each image frame in sequence and the reference (which is fixed). The length of the ROI was fixed to be 2 cm to avoid edge effects. Step 2 is the identification of the instant of fracture within the ROI based on strain data in a color scale, which uses red to represent 0 strain and black to represent strain of 0.1. This scale of 0 (red) to 0.1 (black) was calibrated so that the instant of fracture can be represented by the color of light blue/blue, making it easy to identify. Step 3 is the selection of a secondary region of interest (SROI) from which strain on the failure plane can be obtained.

Output data from the DIC are the average tensile strain and the time of the instant fracture, which was used to identify the load at fracture by matching with the MTS time.

To evaluate the strain distribution along the fracture plane, the SROI was further divided into eleven columns (same length) and corresponding strain data at fracture of each column was collected. Figure 6 indicates that the strain distribution along the fracture surface is nonlinear, with the largest strain at the edges and the lowest strain value at middle of the specimen. The effect of the SROI width on the accuracy of the determined strain was investigated. Figure 6 also shows an SROI width of 0.5 cm resulted in a similar strain distribution on the failure plane as an SROI width of 1.0 cm. Although the larger SROI yielded a smoother strain distribution, the average strain across the fracture surface was almost identical for the two SROI widths (i.e., 0.0293 and 0.0290).

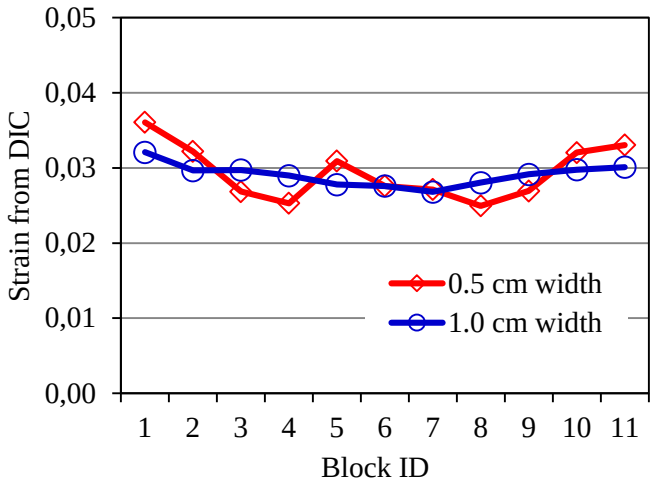

Figure 6. Strain distribution on the fracture surface of a ICDT specimen

Figure 7 reveals a nonlinear correlation between the load-head displacement and average strain. This nonlinearity may be attributed to the induced and re-distributed damage within the specimen throughout the testing process. Of note, both SROI widths (1.0 and 0.5 cm) yielded almost identical correlation between the load-head displacement and average strain values. Thus, the SROI dimension of 1.0 cm in width and 2.0 cm in length was used throughout the analysis of DIC data.

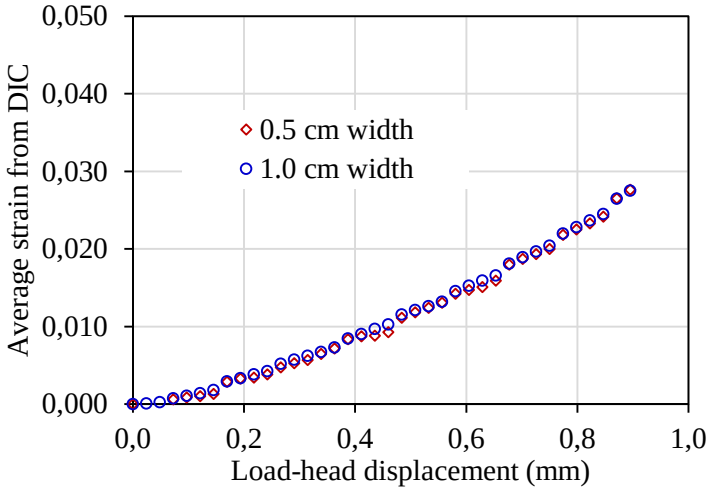

Figure 7. Correlation between average strain and load-head displacement

4.5.2 Strain determination using finite element analysis (FEA)

A previous effort was made to develop a predictive equation for the ICDT test to obtain average local strain based on load-head displacement using the FEA method (43). Due to specimen symmetry, it was only necessary to simulate 1/4 of the specimen with appropriate boundary conditions. The model assumed a linear elastic material with stiffness of 1 MPa and Poisson's ratio of 0.45. The strain field was independent of stiffness and was only affected by the displacement level. The correlation between load-head displacement and average strain on the failure plane (i.e., middle plane) was expressed by Equation 3.

$$y = 0.0199x \quad (3)$$

where, y is the average strain (dimensionless) of the failure plane and x is the load-head displacement (mm).

Results based on the FEA analysis (i.e., average strain, tensile strength and the resulting FED values) were compared to DIC results to determine whether the predictive equation can be used as an alternative to the DIC system.

5. RESULTS AND DISCUSSION

5.1 Repeatability of the ICDT test

An analysis of variance was conducted to evaluate the repeatability of the ICDT tests. Due to the limited number of replicates, a normalization technique was employed. For example, FED of six replicates of a IC type was averaged, and then FED of the individual IC specimen was normalized to that average. This resulted in a population of 48 composted of 8 IC types and 6 replicates per type. Table 3 presents the coefficient of variance (COV), which is the standard deviation divided by the average of the population, determined for normalized tensile strength, failure strain and FED. The DIC method resulted in greater variance in failure strain and FED than the FEA method. This was expected because the DIC method more accurately captured the instant of fracture. Tensile strength was less variable than failure strain and FED and the difference in COV of the tensile strength between the DIC and FEA methods was negligible. Note that the COV of IC FED was within the range reported for the single edge notch bending test (i.e., 3-28%) and the semi-circular bending beam test (15-34%) (44-45).

Table 3. Coefficient of variation of IC fracture properties

Property	Coefficient of variance (%)	
	FEA	DIC
Failure strain (ε_f)	11.8	16.2
Tensile strength (S_t)	5.8	5.8
Fracture energy density (FED)	12.9	16.7

5.2 Evaluation of data interpretation methods

IC fracture properties (i.e., tensile strength, failure strain and FED) obtained from the DIC method were compared to those obtained from the FEA approach. Figure 8 plots the IC tensile strength on average for eight mixtures and it shows that the tensile strength values determined by the DIC and FEM were strongly correlated. The DIC method, which was believed to more accurately capture the instant of fracture, yielded relatively lower tensile strength than the FEA, indicating the instant of fracture occurred slightly before the stress reaching the peak on the FEA stress-strain curve.

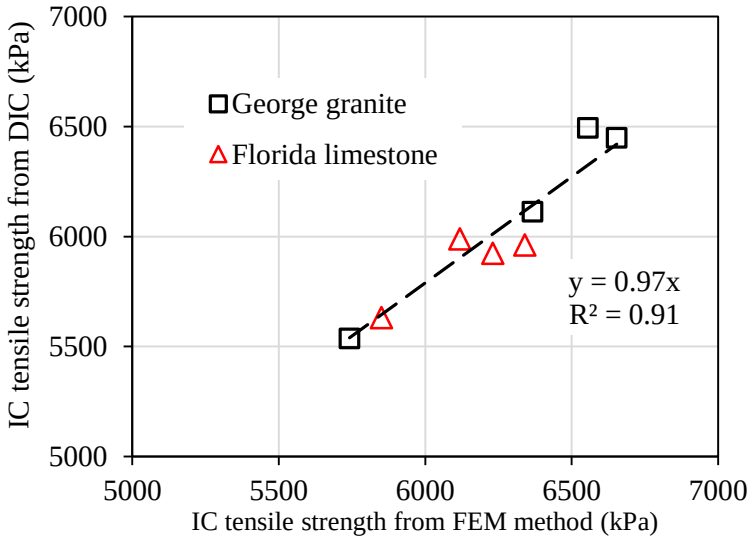

Figure 8. IC tensile strength as determined using the FEA method and the DIC method

As shown in Figure 9, there appeared to be an excellent correlation in failure strain between the DIC and FEA methods. The DIC method yielded greater failure strain values than the FEA method, which was expected because the DIC method more accurately determined the strain on the failure plane whereas the FEA results were obtained from an analysis on non-damaged specimen. Importantly, the DIC strain was consistently 30% greater than the FEA strain of the mixtures evaluated, which allows for estimation of DIC strain based on FEA strain.

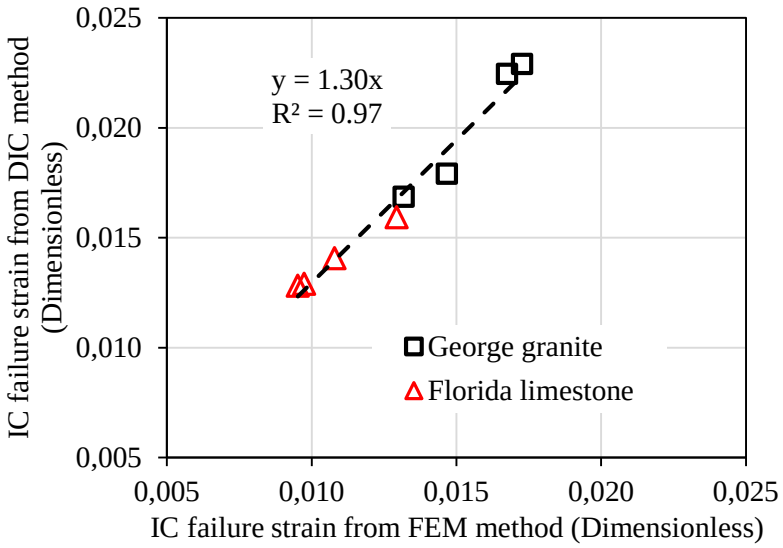

Figure 9. IC failure strain as determined using the FEA method and the DIC method

As a result, IC FED values as determined using the DIC method were strongly correlated (i.e., approximately 32% greater) with those from the FEA method (Figure 10). Although the FEA method yielded lower IC FED values than the DIC method, the underestimation (or the ratio between two strain values) appeared to be consistent for the eight IC types. Therefore, it seems feasible to use the prediction equation of strain from the FEA as a surrogate to the DIC system for determination of IC FED.

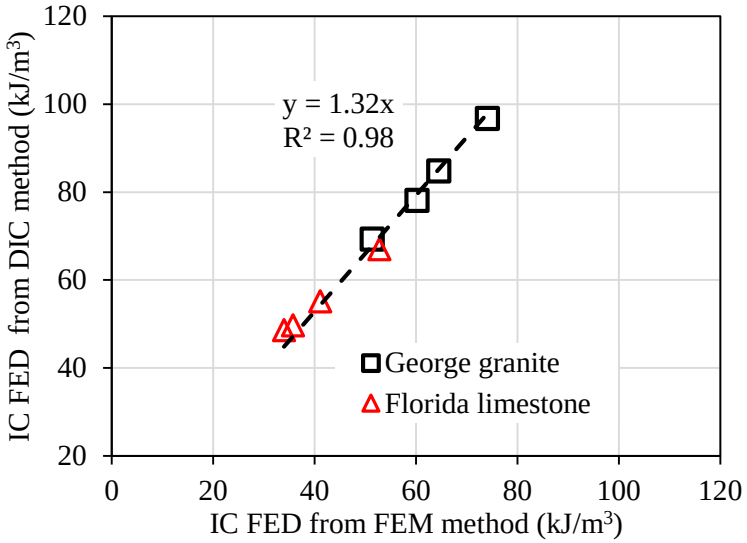

Figure 10. IC FED as determined using the FEA method and the DIC method

5.3 Analysis of correlations between IC FED and mixture FED

A qualitative evaluation of the correlation between IC FED and mixture FED was conducted by normalizing them with respect to the lowest values obtained from FL-IC2. As shown in Figure 11, IC FED distinguished between these mixtures, which had the same coarse aggregate structure but

different composition of IC component. Moreover, IC FED ranked these mixtures in the same order as mixture FED, which substantiates the dominant effect of IC on mixture performance and validates the sensitivity of the newly developed ICDT test to changes in IC composition.

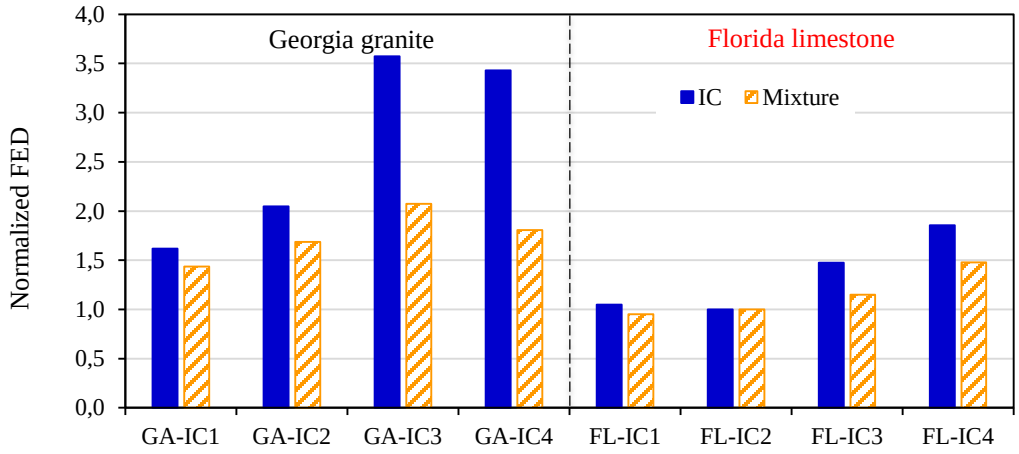

Figure 11. Normalized IC and mixture FED with respect to that of FL-IC2

A quantitative evaluation of the correlation between IC FED and mixture FED was conducted by plotting them against each other. As shown in Figure 12, the IC FED and mixture FED results of the eight mixtures were highly correlated so that the use of a second-order polynomial function with intercept forced to zero satisfactorily fitted these values with the coefficient of determination being 0.90. It is evident that mixture FED is strongly related to IC FED in a positive manner. Figure 12 also reveals that mixture FED increased more rapidly than IC FED as the IC coarseness increased. This may be attributed to the effect of air void content and distribution, which is a mixture level factor that cannot be properly replicated or assessed with the ICDT test.

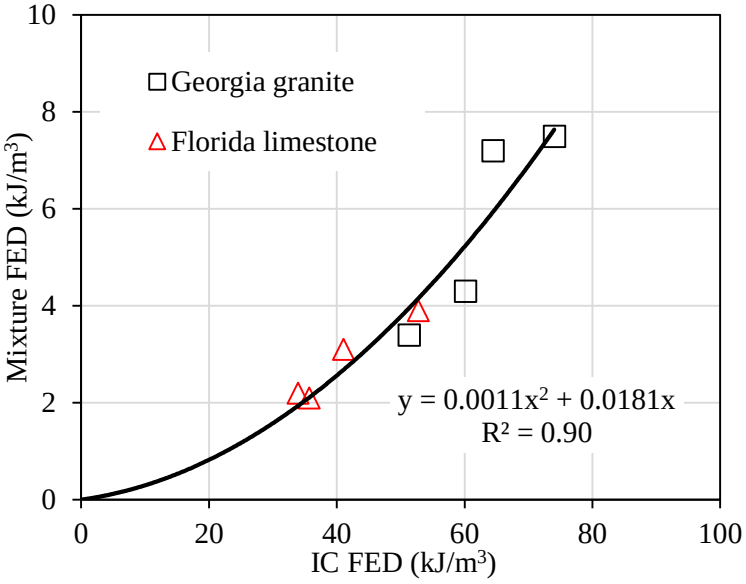

Figure 12. Correlation between IC FED and mixture FED

6. FINDINGS AND CONCLUSIONS

This study employed the ICDT test, which was derived from the DBDT test originally developed for asphalt mixtures, to obtain IC FED at intermediate temperature (10°C). Two methods of strain determination were evaluated including a DIC system and a predictive equation based on FEA analysis. ICDT tests were performed on the IC portion of two sets of four mixtures, whose mixture FED results were available from a previous study. It was of great interest to determine whether IC FED adequately reflects the effect of IC characteristics on mixture FED. Findings are summarized as follows.

- Specimen preparation procedures proposed in this study resulted in ICDT specimens with designed geometry, composition and desired air void content.

- DIC method revealed that local strain nonlinearly distributed on fracture plane with the largest strain obtained from the edge and lowest value from the middle of the specimen.

- DIC method indicated that the average strain exponentially increases with increased load-head displacement, possibly due to the accumulation of damage.

- The ICDT test was found to be repeatable as indicated by the COV of IC fracture properties. DIC method yielded slightly higher COV of failure strain and IC FED than FEA method.

- DIC method resulted in greater IC failure strain and FED values than those based on the FEA predictive equation. More importantly, there appeared to be a constant ratio between DIC strain to FEA strain, as well as between DIC FED and FEA FED.

- IC FED distinguished between eight mixtures and ranked them in the same order as mixture FED. More importantly, an excellent correlation was identified between IC FED and mixture FED results, supporting the relevance and accuracy of IC FED.

Overall, the ICDT test suitably determines the FED of mixture IC portion, which provides valuable insight regarding the effect of IC characteristics on resulting mixture FED. Moreover, the FEA predictive model can be adopted as a surrogate to the DIC system to obtain the IC failure strain. The second-order polynomial function that was used to fit the IC and mixture FED is only valid for the mixtures evaluated in this study. Future work is needed to account for mixture factors (e.g., air voids and coarse aggregate structure), along with IC FED to predict mixture FED. Additional work is also necessary to obtain properties associated with resistance to crack propagation for a more complete assessment of cracking performance at intermediate temperatures.

ACKNOWLEDGEMENT

The authors thank Cristian Cocconcelli, Karl R. Hallstrand and David Hernando for their valuable work during the development and evaluation of this interstitial component direct tension test.

Funding: Not applicable.

Conflict of Interests: The authors declare that they have no conflict of interest.

REFERENCE

1. Soenen, H., De La Roche, C. and Redelius, P. (2004). Predict mix fatigue tests from binder fatigue properties, measured with a DSR, *Proceedings of the 3RD Eurasphalt and Eurobitume Congress*, Vienna, Austria, 12-14th May 2004.
2. Bahia, H.U., Hanson, D.I., Zeng, M., Zhai, H., Khatri, M.A. and Anderson, R.M. (2001). Characterization of modified asphalt binders in Superpave mix design, *NCHRP Report 459*, National Cooperative Highway Research Program, Transportation Research Board —National Research Council, Washington, D.C.
3. Johnson, C.M. (2010). Estimating asphalt binder fatigue resistance using an accelerated test method, *Ph.D. dissertation*, University of Wisconsin-Madison, Madison, WI.
4. Hintz, C., Velasquez, R., Johnson, C. and Bahia, H. U. (2011). Modification and Validation of the Linear Amplitude Sweep Test for Binder Fatigue Specification, *In Transportation Research Record: Journal of the Transportation Research Board*, No. 2207, Transportation Research Board of the National Academies, Washington, D.C., pp. 99–106.
5. Andriescu, A., Hesp, S.A.M. and Youtcheff, J.S. (2004). Essential and plastic works of ductile fracture in asphalt binders, *In Transportation Research Record: Journal of the Transportation Research Board*, No.1875, TRB, National Research Council, Washington, D.C., pp.1–8.
6. Niu, T., Roque, R. and Lopp, G. (2014). Development of a binder fracture test to determine fracture energy properties, *Road Materials and Pavement Design*, Vol.15, Issue.S1, pp.219–238.
7. Yan. Y., Hernando. D. and Roque. R. (2017). Fracture tolerance of asphalt binder at intermediate temperatures, *ASCE Journal of Materials in Civil Engineering*, Vol.29, Issue.9.
8. AASHTO Provisional Standard TP101-14. (2012). Standard method of test for estimating damage tolerance of asphalt binders using the linear amplitude sweep, *American Association of State Highway and Transportation Officials*, Washington, D.C.
9. AASHTO Provisional Standard TP113-15. (2015). Standard method of test for determination of asphalt binder resistance to ductile failure using double-edge-notched (DENT) test, *American Association of State Highway and Transportation Officials*, Washington, D.C.
10. AASHTO Provisional Standard TP127-17. (2017). Standard method of test for determining the fracture energy density of asphalt binder using the binder fracture energy (BFE) test, *American Association of State Highway and Transportation Officials*, Washington, D.C.
11. Rowe, G. (2014). Interrelationships in rheology for asphalt binder specifications, proceedings, 56th Annual Conference, Canadian Technical Asphalt Association, Winnipeg, MB, Canada. pp.457–483.
12. Rowe, G. (2015). Linear visco-elastic binder properties and asphalt pavement cracking, Proceeding of the 11th Conference on asphalt pavements for South Africa (CAPSA15), 16-19th August, Sun City, South Africa, 2015.

13. Rowe, G.M., Sharrock, M.J. and Raposo, S. (2016). Cracking and linear visco elastic binder properties, Proceeding of the *8th RILEM International Conference on Mechanisms of Cracking and Debonding in Pavements*, Nantes, France, 7-9th June 2016.

14. Widyatmoko, I., Elliott, R.C. and Heslop, M.W. (2004). Mapping crack susceptibility of bituminous materials with binder durability, Proceeding of the *5th RILEM International Conference on Cracking in Pavements-Mitigation, Risk Assessment and Prevention*, ENSIL, France, 5-8th May 2004.

15. Rowe, G.M. and Sharrock, M.J. (2016). Cracking of asphalt pavements and the development of specifications with rheological measurements, *Proceeding of the 6th Eurasphalt and Eurobitume Congress*, Prague, Czech Republic, 1-3rd June 2016.

16. Germann, F. P. and Lytton, R. L. (1979). Methodology for predicting the reflection cracking life of asphalt concrete overlays, *Research report FHWA/TX-79/09+207-5*, Texas Transportation Institute, Texas A&M University, College Station, TX.

17. Zhou, F. and Scullion, T. (2003). Upgraded overlay tester and its application to characterize reflection cracking resistance of asphalt mixtures, FHWA/TX-04/0-4467-1, Texas Department of Transportation, Research and Technology Implementation Office, Austin, TX.

18. Mohammad, L.N., Kim, M. and Elseifi, M. (2012). Characterization of asphalt mixtures's fracture resistance using the semi-circular bending (SCB) test, Proceeding of the *7th RILEM International Conference on Cracking in Pavements*, Delft, Netherlands, 20-22nd June 2012.

19. Roque, R. and Buttlar, W. G. (1992). The development of a measurement and analysis system to accurately determine asphalt concrete properties using the indirect tensile mode, *Journal of the Association of Asphalt Paving Technologists*, Vol. 61, pp.304–32.

20. Roque, R., Birgisson, B., Drakos, C. and Dietrich, B. (2004). Development and field evaluation of energy-based criteria for top-down cracking performance of hot-mix asphalt, *Journal of the Association of Asphalt Paving Technologists*, Vol. 73, pp.229–260.

21. Tayebali, A.A., Deacon, J.A., Coplantz, J.S., Harvey, J.T. and Monismith, C.L. (1994). Fatigue response of asphalt-aggregate mixes - Part I test method selection. *Report SHRP-A-404*, Asphalt Research Program, Strategic Highway Research Program, National Research Council, Washington, D.C.

22. Deacon. J.A., Tayebali. A.A., Coplantz. J.S., Finn F.N. and Monismith C.L. (1994). Fatigue response of asphalt - aggregate mixes: Part III mix design and analysis. *Report SHRP-A-404*, Asphalt Research Program, Strategic Highway Research Program, National Research Council, Washington, D.C.

23. Lee, H. J. and Y. R. Kim. (1998). A Viscoelastic continuum damage model of asphalt concrete with healing, *ASCE Journal of Engineering Mechanics*, Vol. 124, No. 11, pp. 1224–1232.

24. Daniel, J. S. and Y. R. Kim. (2002). Development of a simplified fatigue test and analysis procedure using a viscoelastic continuum damage model, *Journal of the Association of Asphalt Paving Technologists*, Vol. 71, pp. 619–650.

25. Wagnoner, M.P.; Buttlar, W.G. and Paulino, G.H. (2005). Disk-shaped compact tension test for asphalt concrete fracture, *Experimental Mechanics*, Vol.45, Issue.3, pp.270–277.

26. Koh, C., Lopp, G. and Roque, R. (2009), Development of a dog-bone direct tension test (DBDT) for asphalt concrete, In: Loizos, A., Partl, M.N., Scarpas, T. and Al-Qadi, I.L. (Eds) *Advanced Testing and Characterization of Bituminous Materials*, Two Volume Set, pp.585–596. London: CRC Press.

27. Luo, X., Luo, R., and R.L. Lytton. (2013). Energy-based mechanistic approach to characterize crack growth of asphalt mixtures, *Journal of Materials in Civil Engineering*, American Society of Civil Engineers, Vol. 25, Issue, 9, pp.1198–1208.

28. Lytton, R., Luo, X., and R. Luo. (2013). A mechanistic empirical model for top-down cracking of asphalt pavement layers, *Interim Report of Project NCHRP 1-52*, Texas A&M Transportation Institute, College Station, TX.

29. Zhou, F., D. Newcomb, C. Gurganus, S. Banihashemrad, M. Sakhaeifar, E.S. Park, and R.L. Lytton. (2016). Experimental design for field validation of laboratory tests to assess cracking resistance of asphalt mixtures. *NCHRP Project. 9-57*. National Cooperative Highway Research Program, the National Academies, Washington, D.C.

30. Di Benedetto, H. and Francken L. (1997). Mechanical tests for bituminous materials, Recent improvements and future prospects, *Proceedings of the Fifth International RILEM Symposium on Mechanical Tests for Bituminous Materials*, Lyon, France, 14-16th May 1997.

31. Di Benedetto, H., de La Roche, C., Baaj, H., Pronk, A.C. and Lundstrom, R. (2004). Fatigue of bituminous mixes: different approaches and RILEM group contribution, *Proceedings of the Sixth International RILEM Symposium on Performance Testing and Evaluation of Bituminous Materials*, Zurich, Switzerland, 11-16th April 2003.

32. Buttlar, W.G., Chabot, A., Dave, E.V., Petit, C. and Tebaldi, G. (2018). Mechanisms of Cracking and Debonding in Asphalt and Composite Pavements: State-of-the-art of the RILEM TC241-MCD, *RILEM State-of-the-Art Reports*, Vol.28, Springer, Switzerland.

33. EN 12697-24 (2018). Bituminous mixtures—Text methods Part 24: resistance to fatigue. *European Committee for Standardization*, Brussels, Belgium.

34. EN 12697-44 (2010). Bituminous mixtures—Test method for hot mix asphalt Part 44: crack propagation by semi-circular bending test. *European Committee for Standardization*, Brussels, Belgium.

35. Haddock, J., Kim, S. and Choubane, B. (1999). Accelerated pavement testing and gradation-based performance evaluation method, *In Transportation Research Record: Journal of the Transportation Research Board*, No.1681, TRB, National Research Council, Washington, D.C., pp.59–68.

36. Ruth, B.E., Roque, R. and Nukunya, B. (2002). Aggregate gradation characterization factors and their relationships to fracture energy and failure strain of asphalt mixtures, *Journal of the Association of Asphalt Paving Technologists*, Vol. 71, 310–344.

37. Kim, S., Roque, R., Birgisson, B. (2006). Identification and assessment of the dominant aggregate size range (DASR) of asphalt mixture. *Journal of the Association of Asphalt Paving Technologists*, Vol. 75, pp.789–814.

38. Guarin, A. (2009). Interstitial component characterization to evaluate asphalt mixture performance, Ph.D. Dissertation, University of Florida, Gainesville, FL.

39. Isola, M. (2014). Effect of interstitial volume characteristics on asphalt mixture durability and cracking performance, *Ph.D. Dissertation*, University of Florida, Gainesville, FL.

40. Bekoe, M.A. (2015). Interstitial component characteristics and its effect on mixture properties, *Ph.D. Dissertation*, University of Florida, Gainesville, FL.

41. Koh, C. and Roque, R. (2010). Use of nonuniform stress-state tests to determine fracture energy of asphalt mixtures accurately, *In Transportation Research Record: Journal of the Transportation Research Board*, No.2181, TRB, National Research Council, Washington, D.C., pp.55–66.

42. Romeo, E. (2013). Two-dimensional digital image correlation for asphalt mixture characterization: interest and limitations, *Road Materials and Pavement Design*, Vol. 14, Issue 4, pp.747–763.

43. Yan, Y., Roque, R., Hernando, D. and Lopp, G. (2017). Development of a new methodology to effectively predict the fracture properties of RAP mixtures, *Road Materials and Pavement Design*, Vol.17, Issue.S4, pp.372–387.

44. Mobasher, B.M., Mamlouk, M.S. and Lin, H-M, Evaluation of crack propagation properties of asphalt mixtures, *ASCE Journal of Transportation Engineering*, Vol.123, pp.405–413.

45. Li, X. and Marasteanu, M. (2004). Evaluation of the low temperature fracture resistance of asphalt mixtures using the semi-circular bend test, *Journal of the Association of Asphalt Paving Technologists*, Vol. 73, 401–426.